Dynamics of Bulk Polyethylene on a High Coordination Lattice

Pemra Doruker and Wayne L. Mattice*

Institute of Polymer Science, University of Akron, Akron, OH 44325-3909, USA

SUMMARY: Monte Carlo simulations of bulk polyethylene were performed on a high-coordination lattice. In this study, we investigated the effect of coarse-grained short and long range interaction parameters on the dynamic properties of the bulk system. As a result of fine tuning of the simulation parameters, our coarse-grained simulations were successful in mimicing the local and large-scale dynamics of $C_{44}H_{90}$ and $C_{100}H_{202}$ melts.

Introduction

A high coordination lattice, which is formed by connecting every other site on a diamond lattice, proved to be a suitable medium for the simulation of various polymers, such as polyethylene (PE),[1-3] polyoxyethylene[4] and polypropylene.[5] This coarse-grained lattice is identical to the hexagonal packing of hard spheres. However, a special name 'the second nearest neighbor diamond (2nnd) lattice' is attributed to it in these specific simulations to emphasize the underlying diamond lattice, from which it originates.[6,7] In these simulations, the rotational isomeric state (RIS) models,[8,9] that describe the statistics of polymer chains in theta conditions, are used to model the local conformational preferences, depending on the chemical structure of the polymers. The long range and intermolecular interactions are incorporated by coarse-graining the Lennard-Jones type interactions on the lattice.

 CCC 1022-1360/98/$ 17.50

During the course of Monte Carlo simulations on the 2nnd lattice, it is also possible to reverse-map any coarse-grained conformation back to the atomistic model in continuous space.[3] This is achieved by performing an energy minimization after replacing the missing atoms on the 2nnd lattice. Reverse-mapped and relaxed snapshots from bulk PE simulations indicated that the local structural and energetic properties of these structures conform with expected values.[3] These results indicate that 2nnd simulations can produce large equilibrated cells of bulk polymers.

Thin film simulations of PE melts were also performed on the 2nnd lattice.[10] Local equilibrium properties are in conformity with atomistic simulations performed for shorter alkanes and the energetics of the films are in agreement with experimental values.

In view of these prior results, our aim here is to study the dynamics of bulk PE simulations on the 2nnd lattice. In these simulations, only single bead moves are performed resulting in local conformational changes. We would like to answer the question of how well these local moves represent the dynamics of the systems. We will discuss how different simulation parameters affect the system dynamics. Our results will also be analyzed in line with some recent molecular dynamics (MD) simulations performed with bulk $C_{44}H_{90}$[11-13] and $C_{100}H_{202}$.[14,15]

Model and Method

The coarse-grained 2nnd lattice, which has a coordination number of 12, is shown in Fig. 1. The center bead and its 12 first neighbors are connected by dark lines on the figure. In the case of PE simulations, each lattice site accommodates two backbone carbon atoms and the hydrogens bonded to them, i.e. a (CH_2CH_2) unit for the internal beads. The lattice

spacing is 2.5 Å, since the length a C-C bond is 1.53 Å and a C-C-C bond angle is tetrahedral on the underlying diamond lattice.

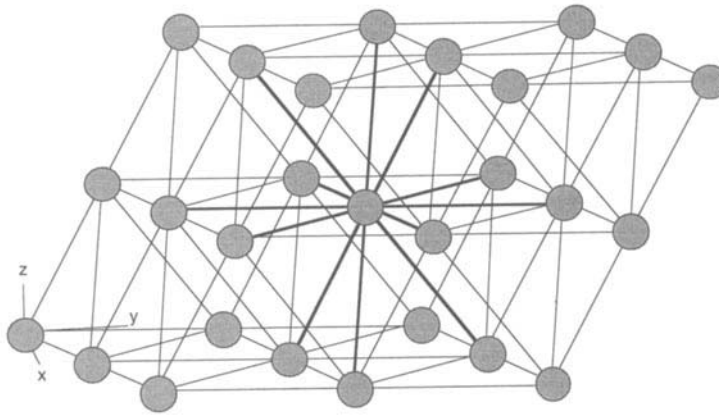

Fig. 1: The coarse-grained 2nnd lattice. Its unit cell is a distorted cube in x,y,z directions

The short range interactions for PE are implemented using the RIS model of Abe et al.[16] There are four coarse-grained states on the 2nnd lattice, which are distinguished by the distance between every other bead. Therefore, the common three-state RIS model for PE,[16] which uses *trans*, *gauche+* and *gauche-* states, has been modified for the coarse-grained states on the 2nnd lattice. The modified statistical weight matrix has the following form

$$U = \begin{bmatrix} 1 & 4\sigma & 2\sigma^2 & 2\sigma^2\omega \\ 1 & 4a & 2b\sigma & 2b\sigma\omega \\ 1 & 4b & 2c & 2c\omega \\ 1 & 4b & 2c & 2c\omega \end{bmatrix} \quad (1)$$

For details of the derivation of the above matrix, ref. 1 should be consulted. Here, σ and ω are the first and second order statistical weights in the original RIS model,[16] respectively. The statistical weights a, b and c result from the coarse-graining procedure and can be used as adjustable parameters, in order to obtain the correct unperturbed chain dimensions, as explained in ref. 7. In the original model of Abe et al., [16] the first and second order interaction energies E_σ and E_ω are given in the respective ranges of (1.8 - 2.5) and (7.1 - 8.0) kJ/mol.[17]

Table 1. Coarse-grained RIS Matrix Parameters for PE

Model	E_σ kJ/mol	E_ω kJ/mol	σ	ω	a	b	c
R1	2.1	8.4	0.532	0.080	$\sigma\,\omega^{1/8}$	$\sigma\,\omega^{1/4}$	$\sigma^2\,\omega^{1/2}$
R2	1.9	7.6	0.56	0.103	0.28	0.168	0.0314
R3	2.7	14.6	0.44	0.0124	$\sigma\,\omega^{1/8}$	$\sigma\,\omega^{1/4}$	$\sigma^2\,\omega^{1/2}$

Table 1 summarizes the short range interaction parameters used in our simulations. Model R1 uses the original parameters from ref. 1. Models R2 and R3 have been modified in order to obtain more realistic characteristic ratios for PE chains, as will be indicated in the results. The temperature dependent σ and ω values are calculated from the first and second order interaction energies at 400 K. In models R1 and R3, a, b and c are calculated as geometric averages of the coarse-grained states and are temperature dependent. In contrast, a, b and c are used as adjustable parameters in model R2. In the simulations

carried out with R2, all parameters σ, ω, a, b and c are held fixed at the values given in Table 1, independent of temperature.

Table 2. Long range interaction energy parameters used in PE simulations

Model	LJ parameters [a]		2nnd lattice shell energies (kJ/mol) [b]				
	ε/k (K)	σ (Å)	u_1	u_2	u_3	u_4	u_5
L1	205	4.2	12.501	0.084	-0.611	-0.137	-0.036
L2	185	4.4	14.122	0.526	-0.627	-0.155	-0.041

[a] Parameters for the Lennard-Jones (LJ) potential.[2,3]
[b] Long range interaction energies for the first five shells on the 2nnd lattice (u_1, u_2 ... u_5), derived from LJ parameters (ε and σ) at 443 K.

The long range interactions among non-bonded units are obtained by an averaging procedure of the Lennard-Jones interactions among ethylene units, since each coarse-grained bead represents a (CH_2CH_2) unit. The details of this averaging procedure are given in ref. 2, which employs the formalism for the second virial coefficient of imperfect gases (Mayer f function) to determine average interaction energies among the neighboring lattice sites. The two sets of long range parameters used for PE in this study are given in Table 2. As can be observed, the interaction energy is highly repulsive for the first shell neighbors, close to zero for the second shell and attractive for the third shell neighbors, in the case of PE. In some simulations, the long range parameters are set equal to zero in order to observe the effect of only short range interactions. In all simulations, however, there is absolute self- and mutual-avoidance of the beads, i.e. no two beads belonging to

the same or different chains can occupy the same site. Table 3 gives a summary of the different bulk simulation systems, which will be cited in this study.

Table 3. Simulation systems

System	Chain length on lattice	Chain number	No. of cells on lattice	Temp (K)	Density (g/cm^3)
$C_{44}(400)$	22	19	13x13x14	400	0.746
$C_{44}(400)L$	22	45	17x18x18	400	0.759
$C_{44}(450)$	22	21	13x14x15	450	0.714
$C_{100}(509)$	50	36	21x22x22	509	0.746
$C_{316}(473)$	158	25	28x28x28	473	0.760

The simulations are performed by applying single bead moves on the 2nnd lattice. When an internal bead is attempted for a move, there are either one, three or no choices of different locations to move it, depending on the location of its two bonded neighbors. These single bead moves on the 2nnd lattice, in reality, alter the position of either two or three consecutive carbon atoms and make changes in three, four or five backbone torsion angles on the underlying diamond lattice. Ref. 3 gives the details on the specific single bead moves. Each Monte Carlo step (MCS) refers to random attempts of moving all the beads in the system.

Results and Discussion

1. Effect of Simulation Parameters on Chain Dynamics

Simulations are performed using the first system $C_{44}(400)$ in Table 3 to analyze the effect of different simulation parameters in bulk systems. In general, all bulk simulations are first performed with only the short-range RIS parameters for faster partial equilibration of the system. Later, the long-range interactions are incorporated and the first 1-2 million MCS of these simulations are discarded as the equilibration period. Analysis periods are long enough to observe several radii of gyration movement of the chain centers of mass. Dynamic properties are calculated upto the first half of the total trajectories.

Table 4 summarizes the results of independent simulations using different sets of short and long range parameters. The first four entries are simulations performed with R1 parameters from Table 1 and different cases of long range interactions. There are no long range interactions in the first entry (except self- and mutual-avoidance), interactions up to two shells (only repulsive interactions), three shells and four shells, respectively, for the next three entries (parameter set L1). There is not much difference among the overall dimensions of the chains, i.e. mean square end-to-end distance $\langle R^2 \rangle$ and mean square radius of gyration $\langle R_g^2 \rangle$, which is consistent with the mean square dimensions being controlled by the short-range intramolecular interactions. The characteristic ratio, defined as $C_N = \langle R^2 \rangle / (N-1)\, l^2$, changes between 5.0-5.4. Here, (N-1) is the number of C-C bonds of the real chain and l is the C-C bond length of 1.53 Å. Although the static properties of the chains are nearly independent of the choice of long-range interactions in the first four entries of Table 4, the dynamics of the system is affected significantly. Incorporation of the long-range interactions slows down the large scale dynamics. Large scale dynamics is monitored in terms of the chain center of mass diffusion and the chain end-to-end vector reorientation. The long time self diffusion coefficients are tabulated as D_N in Table 4, in units of $Å^2$/MCS. There is almost an order of magnitude decrease in D_N when long range

interactions are added.

The end-to-end vector autocorrelation function of the chains fitted to the Rouse model[18] according to

$$\frac{\langle \mathrm{R}(t)\cdot \mathrm{R}(0)\rangle}{\langle R^2\rangle} = \sum_{p=1,3\ldots} \frac{8}{p^2\pi^2}\exp(-tp^2/\tau_R) \qquad (2)$$

Here, the Rouse time τ_R, which is the longest relaxation time of the chains, is the only adjustable parameter. The sum extends over all odd p values. In our case, the fits are performed with p going up to 7. The values of τ_R are given in Table 4. Again, there is an order of magnitude difference among the relaxation times of the first four entries.

If we compare entries 3 and 5, the effect of different sets of long range parameters (L1 and L2) is observed using the same R1 model. There is almost no difference among the overall dimensions of the chains. However, there is a slowing down of the large scale dynamics (lower D_N and larger τ_R) in the case of the new parameters L2. The parameter set L2 was used in thin film simulations.[10] L2 gives more realistic bulk densities in PE thin film simulations, where the system is free to choose its own density due to the two-dimensional periodic conditions.

The three entries (5-7) in Table 4 indicate how different RIS models affect the simulation results. The R1 model is modified to obtain chains that are more expanded. As the overall dimensions of the chains increase, the large scale dynamics slows down. There is an order of magnitude slowing down from R1 to R3 model, in terms of both the translational diffusion and the end-to-end vector decorrelation of the chains. Entries 8 and 9 are variations performed with R3. Entry 8 has no long range interactions, while entry 9 has only the first repulsive shell of L2.

Table 4. Different coarse-grained runs of C_{44} bulk system at 400 K

Run	Parameter sets [a]	C_N [b]	τ_R (10^4 MCS)	D_N (10^{-4} Å^2 /MCS)	$\tau_R D_N$ (Å^2)	$\zeta(\tau_R)$ / $\zeta(D_N)$	MCS [c] (fs)
1	R1-none	5.4 (79)	0.95	15	14	0.79	171-79
2	R1- L1 (2s)	5.4 (79)	6.42	2.9	19	1.05	25-15
3	R1- L1 (3s)	5.0 (74)	7.5	2.0	15	0.91	22-11
4	R1- L1 (4s)	5.2 (77)	11.5	1.8	21	1.20	14-10
5	R1- L2 (3s)	5.1 (76)	11.4	1.7	19	1.15	14-9
6	R2- L2 (3s)	6.5 (91)	54.6	0.5	27	1.27	3-2.6
7	R3- L2 (3s)	6.9 (95)	168	0.17	29	1.25	1.-0.9
8	R3- none	7.1 (97)	4.75	3.8	18	0.77	34-20
9	R3- L2 (1s)	7.1 (98)	53.5	0.35	19	0.80	3-1.8

[a] Short and long range parameter sets are indicated. The numbers in parenthesis give the number of shells used in the calculation of long range interactions. The term 'none' indicates that the long range parameters are set equal to zero. However, self- and mutual avoidance of the beads are absolute in all simulations.

[b] Numbers in parenthesis are the mean squared radii of gyration (Å^2) of the chains.

[c] This column gives the MCS converted to real time (in fs) by using τ_R and D_N data, respectively, from explicit MD simulations (refer to Table 5)

Fig. 2 gives the mean square displacement of the chains centers of mass divided by 6t as a function of time t, where time is MCS in our simulations. The diffusion coefficients tabulated in Table 4 are calculated from the long time limit, or the plateau value of the curves. Here, the curves are drawn for entries 6 and 7 of Table 4.

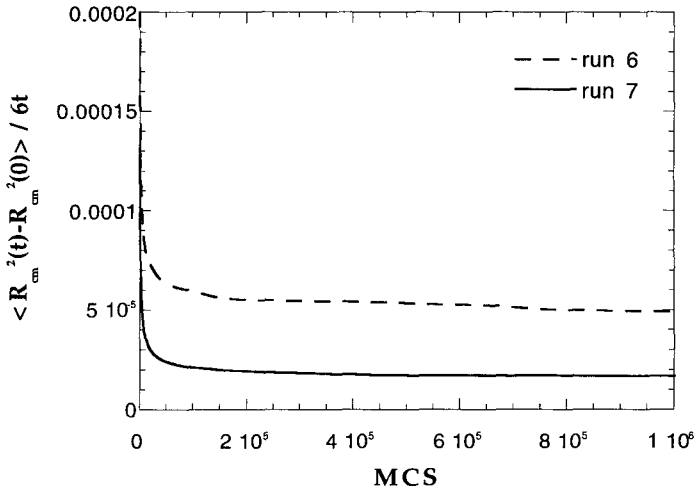

Fig. 2: The mean square displacement of the chain centers of mass divided by 6 (MCS), as a function of MCS for runs 6 and 7

Fig. 3 displays the end-to-end vector autocorrelation function for the same entries 6 and 7 of Table 4 (dark dashed lines) and the corresponding Rouse fits (thinner lines), according to eq. 2. The two types of lines are not easily distinguishable because the Rouse fits are a good description of the data.

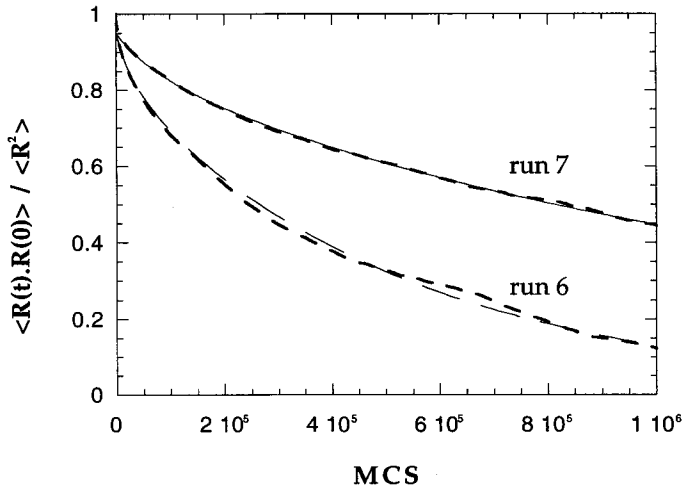

Fig. 3: Chain end-to-end vector autocorrelation functions and the corresponding Rouse fits for runs 6 and 7

Our aim in making these comparisons among the different parameters is to learn how the various parameters in the simulations affect the static and dynamic properties, to determine which parameters best represent the dynamics of PE and to also adjust the parameters so that our simulations are efficient. In terms of efficiency, each Monte Carlo step should correspond to a reasonable real time, when comparison is made with atomistic simulations (This will be done in the next section). Another important issue in terms of efficiency is the total number of shells that will be used for calculating the long range interaction energy in our simulations. Since nonbonded interactions are the most demanding part in the computations, it is important to take into account the least number of shells or none, if possible. With these objectives in mind, we can move on to comparing our results with the atomistic simulations carried out with PE bulk systems.

2. Comparison of C_{44} Chain Dynamics with MD Simulation Results

Explicit atom and united atom MD simulations have been performed with $C_{44}H_{90}$ bulk system at 400 K and 450 K.[11-13] We will first analyze our results from the previous section in view of the system at 400 K. The MD simulations at 400 K are carried out with 45 chains at a density of 0.757 g/cm^3. Our simulations with 19 chains are at a slightly lower density of 0.746 g/cm^3. So we performed another simulation with 45 chains at 0.759 g/cm^3 (C_{44}(400)L in Table 3) to see the effect of system size and density. Table 5 summarizes the results from both explicit and united atom MD simulations and our simulation results. Comparison of systems with 19 and 45 chains with parameter sets R1-L2, we see that there is only a slight slowing down of dynamics in the bigger system due to the increase in density and the overall dimensions are identical. Therefore, it is possible to safely compare the results of the 19 chain runs with MD simulations.

We need some values which are independent of time for comparison, since MD simulation results are in real time, whereas MC simulation results are in MCS. The last two columns in Table 5 (see also Table 4) report τ_R D_N value in Å^2 and the dimensionless ratio of the monomer friction coefficients, $\zeta(\tau_R)$ /$\zeta(D_N)$. The monomer friction coefficient can be obtained independently from the Rouse time or the self-diffusion coefficient, by the following equations, respectively.

$$\zeta(\tau_R) = \frac{3\pi^2 k_B T \tau_R}{N\langle R^2 \rangle}$$

$$\zeta(D_N) = \frac{k_B T}{N D_N} \qquad (3)$$

The monomer friction coefficients obtained by two equations above should be equal, if the chains exhibit Gaussian coil characteristics according to the Rouse model. MD

simulations[12,13] showed that $C_{44}H_{90}$ chains in bulk are not long enough to show Gaussian coil characteristics, so that the $\zeta(\tau_R)/\zeta(D_N) > 1$, as observed in Table 5. If we go back and look at the entries of Table 4, we can see that the closest matches to the MD results are runs 6 and 7, which are again displayed in Table 5.

Table 5. Comparison of MD and MC Simulation Results (C_{44} System at 400 and 450 K)

Simulation	C_N [b]	τ_R (ps, or MCS)	D_N (cm^2/ps, or $Å^2/MCS$)	$\tau_R D_N$ ($Å^2$)	$\zeta(\tau_R)$ / $\zeta(D_N)$
Explicit Atom [a]					
400 K	7.4 (97)	1614	1.9×10^{-6}	30.7	1.23
450 K	7.0 (95)	791	5.4×10^{-6}	42.7	1.79
United Atom [a]					
400 K	7.3 (99)	938	3.5×10^{-6}	32.8	1.29
450 K	7.1 (98)	494	7.0×10^{-6}	34.6	1.43
R1- L2 (3s)					
C_{44}(400)L	5.1 (76)	1.2×10^5	1.5×10^{-4}	17.9	1.00
C_{44}(400)	5.3 (78)	1.14×10^5	1.7×10^{-4}	19.4	1.15
C_{44}(450)	5.2 (76)	5.35×10^4	3.4×10^{-4}	18.1	1.05
R2- L2 (3s)					
C_{44}(400)	6.5 (91)	5.46×10^5	5.0×10^{-5}	27.3	1.27
C_{44}(450)	6.0 (86)	2.66×10^5	7.8×10^{-5}	20.7	1.06
R3- L2 (3s)					
C_{44}(400)	6.9 (95)	1.7×10^6	1.7×10^{-5}	28.6	1.25
C_{44}(450)	5.9 (86)	6.0×10^5	3.5×10^{-5}	21.0	1.07

[a] MD simulation results from ref. 12 (explicit atom) and ref.13 (united atom).
[b] Numbers in parenthesis are the mean squared radii of gyration ($Å^2$) of the chains.

We ran simulations at 450 K, in order to see the effect of temperature. MD simulations[12,13] were performed at a density of 0.728 g/cm^3, which is slightly higher than the density of our system C_{44}(450). The results in Table 5 indicate that both self-diffusion and end-to-end vector reorientation dynamics of the chains are enhanced at the higher temperature. However, the effect is not as strong as that observed in MD simulations, if we compare the reported values of τ_R D_N and $\zeta(\tau_R)$ /$\zeta(D_N)$. This might partly result from the significant decrease in overall dimensions due to temperature in coarse-grained simulations, which is not seen in MD simulations.

We could also look at local dynamics at the time scale of the relaxation of the 2nnd bonds on the lattice, which correspond to the C-C-C chord vector on the backbone of atomistic chains. In the explicit atom MD simulations,[12] the orientation autocorrelation function (OACF) of this chord vector is fitted to a modified Kohlrausch-Williams-Watts (MKWW) equation, as below

$$P(t) = A\exp[-(t/\tau)^{\beta}] + (1-A)\exp(-t/\tau_{tail}) \qquad (4)$$

Here, P(t) is the first Legendre polynomial for the C-C-C chord vector. The modification is the additional exponential term which describes the long time behavior of the decay. Fig. 4 gives the OACF decay for the chord vector of run 6 (dark dashed line) and the corresponding MKWW fit (thinner line). Table 6 summarizes the numerical results from explicit atom MD and coarse-grained simulations. The fits seem to be in reasonable agreement.

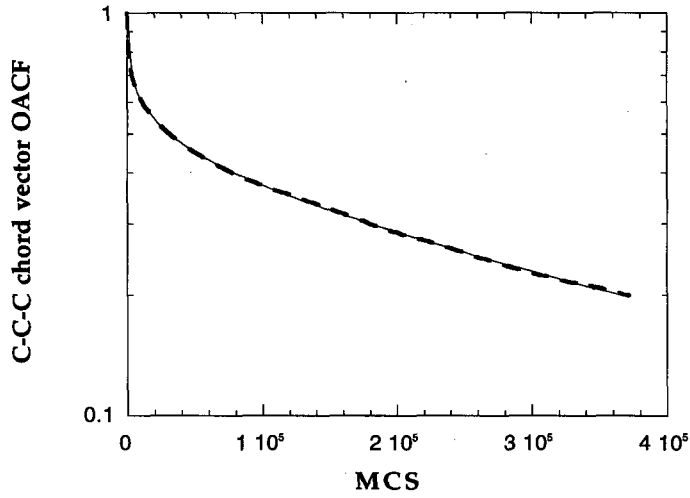

Fig. 4: C-C-C chord vector orientation autocorrelation function and the corresponding MKWW fit for run 6

Table 6. MKWW fits to the C-C-C chord vector OACF. (C_{44} System at 400 K)

Simulation	τ (ps, or MCS)	τ_{tail} (ps, or MCS)	β	A	τ/τ_R
Explicit Atom[a]	30.8	916	0.50	0.542	0.025
R1- L2 (3s)	4.49×10^3	2.14×10^5	0.37	0.564	0.039
R2- L2 (3s)	1.56×10^4	5.33×10^5	0.35	0.670	0.029
R3- L2 (3s)	3.83×10^4	1.26×10^6	0.39	0.546	0.023

[a] data from ref. 12.

3. Comparison of C_{100} Chain Dynamics with MD Simulation Results

Explicit atom and united atom MD simulations have been performed with bulk $C_{100}H_{202}$ at 509 K.[14] The results on large scale dynamics are mainly from the united atom simulation (duration of 9 ns) in ref. 14, since the explicit atom simulation is much shorter (1.1 ns). The results of MD simulations and our coarse-grained simulations are reported in Table 7. The density of the bulk system is 0.746 g/cm^3 at 509 K. The Rouse model fits are performed with p going up to 13, according to eq. 2. The results on large scale dynamics seems to be closer to MD results in the case of R1 and R3 compared to R2, even though the overall dimensions of chains with R2 is really close to expected values.

Table 7. Comparison of MD and MC Simulation Results (C_{100} System at 509 K)

Simulation	C_N [b]	τ_R (ps or MCS)	D_N Å^2/(ps or MCS)	$\tau_R D_N$ (Å^2)	$\zeta(\tau_R)$ / $\zeta(D_N)$
United Atom [a]	7.2 (256)	2090	0.26	54.3	0.95
R1- L2(3s)	4.9 (181)	2.53×10^5	1.5×10^{-4}	40.0	1.05
R2- L2 (3s)	7.2 (248)	3.89×10^6	1.8×10^{-5}	70.0	1.26
R23- L2 (3s)	6.2 (228)	2.30×10^6	2.0×10^{-5}	46.0	0.95

[a] data from ref. 14.
[b] Numbers in parenthesis are the mean squared radii of gyration (Å^2) of the chains.

In order to analyze the time scales of local dynamics, the autocorrelation time, τ_{ccc}, is calculated by integrating the OACF decay (the first Legendre polynomial) of the C-C-C chord vector. τ_{ccc} is reported as 288 ps for the united atom MD in ref. 14. The ratio of τ_{ccc}/τ_R is used for comparison with our MC results. Thus, τ_{ccc}/τ_R equals to 0.14 (united atom), 0.19 (R1-L2), 0.74 (R2-L2) and 0.22 (R3-L2).

The self diffusion behavior of the chains is displayed in the form of five different mean-square displacements (m.s.d.) in ref. 14. These can be summarized as follows: g_1 (the m.s.d. of the center monomers of the chains), g_2 (the m.s.d. of the center monomers in the chain center of mass reference frame), g_3 (the m.s.d. of chain centers of mass), g_4 (the m.s.d. of the end monomers of the chains) and g_5 (the m.s.d. of the end monomers in the chain center of mass reference frame). Fig. 5 gives the behavior of these five mean-square displacements for the coarse-grained simulation performed with parameter set R1-L2. The behavior is similar to that obtained with the united atom MD simulation. Monomer mean-square displacements exhibit a subdiffusive regime, where g_1 and g_4 are almost proportional to $t^{1/2}$ (t is in MCS) before passing to free diffusion for $t > \tau_R$, as predicted by the Rouse model.[18] (The subdiffusive coefficients for g_1 and g_4 are 0.57 and 0.58, respectively.) On the other hand, g_2 and g_5 level off to a plateau, since they are measured in the center of mass reference frame of the chains. The center of mass diffusion also displays a subdiffusive regime, where g_3 is proportional to $t^{0.87}$ for $t < \tau_R$ and passes slowly to the Fickian behavior in the long time limit. The same situation is observed in the MD simulations,[14] as well as other prior coarse-grained simulations.[19,20] The diffusion coefficients reported for C_{100} (and also for C_{44} in the previous section) are extracted from the long time, $t > \tau_R$ region.

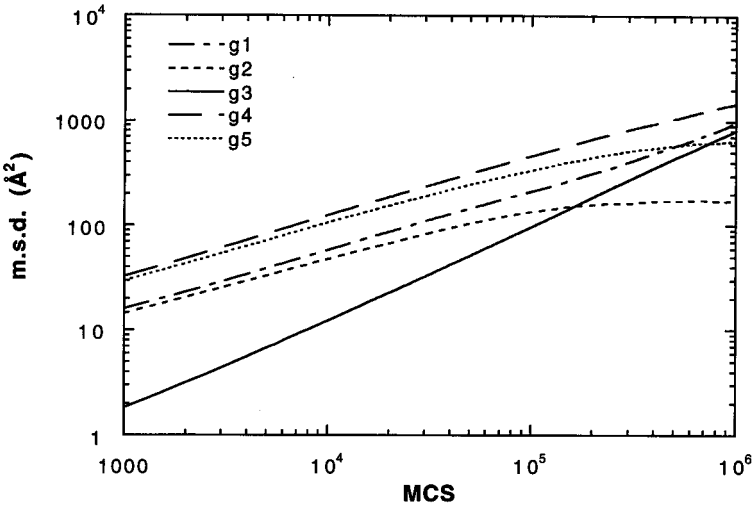

Fig. 5: Mean square displacements of the chain centers of mass, middle and end beads (see text for details) as a function of time for C_{100} (R1-L2)

Relaxation times have been defined on the basis of different mean square displacements in previous work,[19] as follows:

$$
\begin{aligned}
g_1(\tau_1) &= \langle R_G^2 \rangle \\
g_2(\tau_2) &= \frac{2}{3}\langle R_G^2 \rangle \\
g_3(\tau_3) &= g_2(\tau_3) \\
g_5(\tau_4) &= \langle R_G^2 \rangle
\end{aligned}
\qquad (5)
$$

The relaxation times extracted from Fig. 5 are listed in Table 8, together with MD results. The ideal Rouse model predicts $\tau_4 << \tau_2 \leq \tau_1 << \tau_3$, with a 20 % difference between τ_1 and τ_2.[14,19] Moreover, ref. 19 reports the following ratios for $\tau_3/\tau_1 = 3.112$ and $\tau_4/\tau_1 =$

0.279. In our simulations performed with R1 and R3, the ordering and magnitudes of the relaxation times seem reasonable. However, in the case of R2 we get a peculiar ordering of the relaxation times with τ_2 being the longest one.

Table 8. Comparison of MD and MC Simulation Results (C_{100} System at 509 K)

Simulation	τ_1	τ_2	τ_3	τ_4	τ_3/τ_1	τ_4/τ_1
	ns, or 10^4 MCS					
United atom [a)]	0.61	0.75	1.24	0.49	2.03	0.80
R1- L2 (3s)	7.25	6.85	16.5	2.65	2.28	0.37
R2- L2 (3s)	109	171	150	32.2	1.38	0.30
R3- L2 (3s)	88.6	88.9	198	23.8	2.23	0.27

[a)] data from ref. 14.

4. Efficiency of the MC Simulations

The efficiency of our MC simulations depends on two parameters: (i) ratio of CPU time required for the execution of a single MC step to that of an MD step, and (ii) the conversion between a MC step and real time measured in seconds. To account for the first issue, we performed both MD and MC simulations of the same number of steps on the same SGI workstation. The system consisted of nine chains of $C_{100}H_{202}$ at a density of 0.86 g/cm^3, in both simulations. The MD simulation was performed with a commercial software package using 1 fs time steps. In MC simulations, long range interactions are counted upto three shells, which is the preferable case in most PE simulations. The ratio

of MC to MD CPU times is ~ 35. The second issue of converting a MC step to real time, depends primarily on the specific short and long range parameter sets that we employ. For example, we can see in the last column of Table 4, the real time counterpart of MCS, extracted from the comparison of τ_R and D_N values with the explicit atom model results. Our efficiency will be determined by the specific model we choose. In fact, the time scales of the dynamics of explicit and united atom MD simulation are quite different in Table 5, from which we extract the real time of a MCS. In our conversions in Table 4, we used the explicit atom model.

In view of the above discussions, incorporation of long range interactions decreases the efficiency of the simulations due to two reasons. The CPU time of a MCS increases significantly due to extensive calculations. Moreover, the dynamics of the coarse-grained bulk systems slows down, so that the real time, to which a MSC corresponds, decreases. Therefore, it is desirable to carry out simulations with only short range interactions to gain efficiency in cases of equilibration, where the dynamics of the system is not of interest. Long range interactions could, later on, be added to the simulations.

5. Linear vs. Cyclic Chain Dynamics

In this section, we will discuss the large scale dynamics of preliminary simulations performed with C_{100} and C_{316} bulk systems. Both linear and cyclic chains have been simulated with R1 parameters and no long range interactions (except self- and mutual-avoidance). Our aim, here, is to see if there is any slowing down in the mean square displacements due to entanglements in the case of longer linear chains.

Fig. 6 displays the g_1 and g_3 for C_{100} cyclic chains (thin dashed lines) and g_1, g_3 and g_4 for linear chains (dark lines). The mean square radii of gyration for the cyclic and linear chains are 88 and 180 $Å^2$, respectively. We cannot observe any significant difference among the m.s.d.'s of cyclic and linear chains. The exponents of the different regimes for linear

chains are indicated on the figure. In the long time limit, we clearly see that g_1 and g_3 exhibit free diffusion with exponents ~ 1.0.

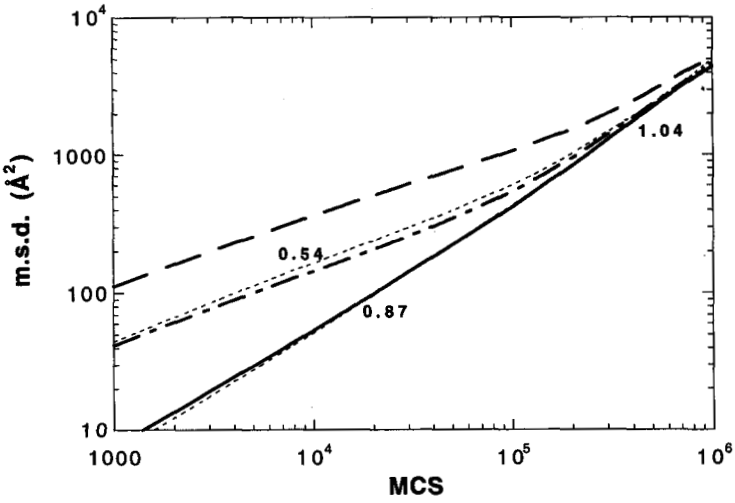

Fig. 6: Mean square displacements for cyclic and linear chains of C_{100}

In Fig. 7, g_1 and g_3 are plotted for C_{316} cyclic (dashed lines) and linear (solid lines) chains. The mean square radii of gyration for the cyclic and linear chains are 269 and 649 $Å^2$, respectively. Although the dynamics of cyclic chains are comparatively faster due to smaller size, we can still observe the difference in the exponents of the m.s.d's in the figure. In the subdiffusive regime, $g_1 \sim t^{0.50}$ and $g_3 \sim t^{0.88}$ for cyclic chains, whereas, the exponents drop down to 0.39 and 0.79, respectively, for linear chains.

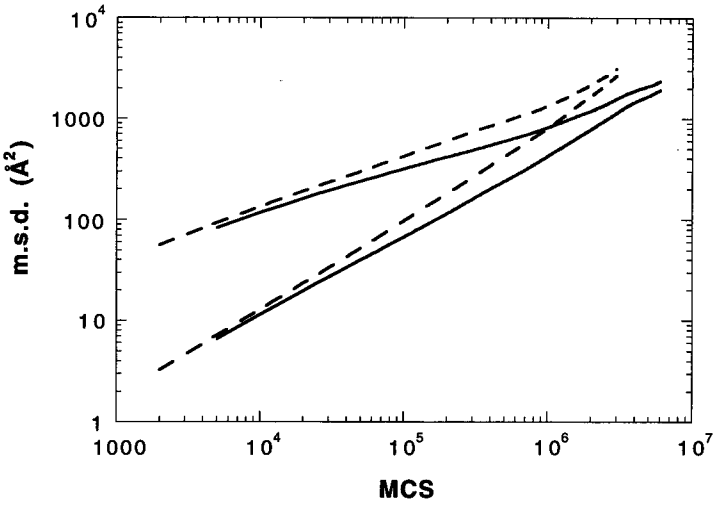

Fig. 7: Mean square displacements for cyclic and linear chains of C_{316}

Concluding Remarks

Among the RIS models investigated, R3 represents the equilibrium and dynamic properties of PE most successfully. However, in terms of efficiency, R1 is the most efficient, but gives quite collapsed chains. Model R2 is not suitable for representing the $C_{100}H_{202}$ dynamics. In terms of long range interactions, models L1 and L2 are both suitable for representing the bulk system. In this study, model L2 was used more extensively, since it was found to be more successful in prior simulations of PE thin films.[10] In general, long range interactions could be omitted for gain in efficiency during the initial stages of equilibration. However, they should be implemented upto three shells

for best representation of PE properties. Combination of models R3 and L2 was successful in representing $C_{44}H_{90}$ and $C_{100}H_{202}$ melt dynamics at 400 K and 509 K, respectively. However, the temperature dependence of the RIS model for the short chains did not fit the MD simulations results.

Acknowledgment

This work was supported by National Science Foundation grant DMR 9523278.

References

[1] R. F. Rapold, W. L. Mattice, *Macromolecules* **29**, 2457 (1996)

[2] J. Cho, W. L. Mattice, *Macromolecules* **30**, 637 (1997)

[3] P. Doruker, W. L. Mattice, *Macromolecules* **30**, 5520 (1997)

[4] P. Doruker, R. F. Rapold, W. L. Mattice, *J. Chem. Phys.* **104**, 8742 (1996)

[5] T. Haliloglu, W.L. Mattice, *J. Chem. Phys.* (in press)

[6] R. F. Rapold, W. L. Mattice, *J. Chem. Soc. Faraday Trans.* **91**, 2435 (1995)

[7] I. Bahar, J. Cho, P. Doruker, B. Erman, T. Haliloglu, E.-G. Kim, W. L. Mattice, L. Monnerie, R.F. Rapold, *Trends in Polym. Sci.* **5**, 155 (1997)

[8] P. J. Flory, *"Statistical Mechanics of Chain Molecules"*, Wiley, New York, 1969

[9] W. L. Mattice, U. W. Suter, *"Conformational Theory of Large Molecules. The Rotational Isomeric State Model in Macromolecular Systems"*, Wiley, New York, 1994

[10] P. Doruker, W. L. Mattice, *Macromolecules* **31**, 1418 (1998)

[11] G. D. Smith, D. Y. Yoon, W. Zhu, M. D. Ediger, *Macromolecules* **27**, 5563 (1994)

[12] G. D. Smith, D. Y. Yoon, R. L. Jaffe, *Macromolecules* **28**, 5897 (1995)

[13] W. Paul, D. Y. Yoon, G. D. Smith, *J. Chem. Phys.*, **103**, 1702 (1995)

[14] W. Paul, G. D. Smith, D. Y. Yoon, *Macromolecules* **30**, 7773 (1997)

[15] G. D. Smith, W. Paul, D. Y. Yoon, A. Zirkel, J. Hendricks, D. Richter, H. Schober, *J. Chem. Phys.* **107**, 4751 (1997).

[16] A. Abe, R. L. Jernigan, P.J. Flory, *J. Am. Chem. Soc.* **88**, 631 (1966)

[17] M. Rehahn, W. L. Mattice, U. W. Suter, *Advances in Polym. Sci.* **131/132**, 464 pp (1997)

[18] P. E. Rouse, *J. Chem. Phys.* **21**, 1272 (1953).

[19] W. Paul, K. Binder, D. W. Heermann, K. Kremer, *J. Chem. Phys.* **95**, 7726 (1991)

[20] K. Kremer, G. S. Grest, *J. Chem. Phys.* **92**, 5057 (1990)